Hindawi
Shock and Vibration
Volume 2021, Article ID 9954098, 14 pages
https://doi.org/10.1155/2021/9954098

Research Article

Research on Vibration Law of Railway Tunnel Substructure under Different Axle Loads and Health Conditions

Weibin Ma,[1,2] **Jinfei Chai**,[1,2] **Zifeng Zhu**,[3] **Zili Han**,[1,2] **Chaofeng Ma**,[1,2] **Yuanjun Li**,[4,5] **Zhenyu Zhu**,[6] **Ziyuan Liu**,[1,2] **Yabin Niu**,[1,2] **Zhanguo Ma**,[1,2] **Mu Gu**,[1,2] **Guoqiang Zhang**,[4,5] **Cheng Li**,[7] **and Sen Zhang**[8]

[1]*Railway Engineering Research Institute, China Academy of Railway Sciences Corporation Limited, Beijing 100081, China*
[2]*State Key Laboratory for Track Technology of High-speed Railway, Beijing 100081, China*
[3]*School of Mathematics and Science, Beihang University, Beijing 102206, China*
[4]*China Railway Taiyuan Bureau Group Corporation Limited, Taiyuan, Shanxi 030013, China*
[5]*Datong-Qinhuangdao Railway Corporation Limited, Taiyuan, Shanxi 030000, China*
[6]*Beijing Railway Signal Corporation Limited, Beijing 100071, China*
[7]*Hohhot Engineering Section, China Railway Hohhot Bureau Group Corporation Limited, Jining, Inner Mongolia 010051, China*
[8]*Beijing Tieke Special Engineering Technology Corporation Limited, Beijing 100081, China*

Correspondence should be addressed to Jinfei Chai; chaijinfei@rails.cn and Zili Han; 903443989@qq.com

Received 23 April 2021; Accepted 4 June 2021; Published 28 June 2021

Academic Editor: Chengwei Fei

In this paper, 25-ton and 27-ton axle heavy trucks are used to carry out moving loading and dynamic real vehicle test on the cracked section, the intact section, and the repaired section of a railway tunnel foundation to test the dynamic performance of the tunnel basement structure with the change of axle loads and health conditions. By analyzing the influence law of dynamic response and fatigue life of heavy haul train under different basement conditions (intact, damaged, and repaired), the adaptability of railway tunnel equipment to freight trucks axle load is clarified. The results show that (1) the intact section of the tunnel can meet the normal operation of 25-ton and 27-ton axle load freight trains in good condition. (2) The normal operation of 25-ton and 27-ton axle load freight trucks is seriously affected by the cracked section of the tunnel. When the cracks in the tunnel basement are gradually hollowed out by groundwater, serious traffic accidents such as vehicle shaking and derailment are likely to occur. (3) The repaired section of the tunnel can meet the normal operation of 25-ton and 27-ton axle load freight trains after adopting the integrated comprehensive treatment of "Anchor-Injection-Drainage". The research results will have reference significance for the condition assessment and disease treatment of the basement structure of the heavy haul railway tunnel.

1. Introduction

Heavy haul railway has become the best choice for transporting bulk goods in the world because of its advantages of large volume, high speed, low energy consumption, and low cost. However, it is inevitable that heavy haul railway tunnels under construction and completed will inevitably have greater hidden dangers due to the bearing of heavy train load on the foundation structure. Lots of scholars have researched the stress distribution characteristics and dynamic response of heavy haul railway tunnel structure under heavy train load [1–15]. But there is still insufficient understanding of the vibration characteristics of substructure of the heavy haul railway tunnel under different axle loads and health conditions. Therefore, it is of great significance to study the vibration characteristics for the basement structure of heavy haul railway tunnel under different axle loads and health conditions.

There are many railway tunnels in China, and most of them are long tunnels [16]. Under the condition of running 10,000-ton and 20,000-ton C80 freight trucks, some structural defects gradually appear in the railway tunnel, especially the basement crack damage, the tunnel construction joints, variable cross section of refuge tunnel, and leakage water, and are particularly obvious. In addition, the problems of drainage system blockage, ditch silting, water accumulation at the tunnel basement structure, and pressure bearing are also prominent [17].

2. Dynamic Stress and Vibration Response of Tunnel Basement Structure

In this paper, 25-ton and 27-ton axle heavy trucks are used to carry out moving loading and dynamic real vehicle test on the cracked section, the intact section, and the repaired section (adopting the integrated comprehensive treatment of "Anchor-Injection-Drainage") of a railway tunnel foundation. The dynamic pressure stress and vibration acceleration of the tunnel basement structure under the action of 25-ton and 27-ton axle load freight trucks under different health conditions are analyzed. The load characteristics of the foundation of the typical section of the existing railway tunnel under the operation conditions of 25-ton and 27-ton axle load freight trucks as well as the stress and vibration laws of the foundation structure are mastered. It provides the measured data for the stress checking and evaluation of the foundation structure in the typical section of the existing railway tunnel.

2.1. Test Content. The dynamic test was carried out to test the dynamic performance of the tunnel basement structure with the change of axle loading and health conditions.

(1) Dynamic response and adaptability analysis of typical railway tunnel basement structure to C80 (25-ton axle load) and C80E (27-ton axle load) freight trucks under the condition of intact tunnel basement structure

(2) Dynamic response and adaptability analysis of typical railway tunnel basement structure to C80 (25-ton axle load) and C80E (27-ton axle load) freight trucks under tunnel basement structure cracking condition

(3) Dynamic response and adaptability analysis of typical railway tunnel foundation structure to C80 (25-ton axle load) and C80E (27-ton axle load) freight trucks under the condition of tunnel basement structure crack damage anchorage reinforcement

2.2. Test Method. The test methods used in this paper are as follows:

(1) Dynamic stress test of tunnel basement structure: dynamic stress sensors are installed at different positions on the concrete surface of the filling layer, and a dynamic acquisition instrument is used to monitor the dynamic strain of concrete on the surface of the filling layer when the train passes through the tunnel

(2) Vibration acceleration test of tunnel basement structure: vibration acceleration sensors are installed at different positions on the concrete surface of the filling layer, and a dynamic acquisition instrument is used to monitor the vibration acceleration of filling layer surface when the train passes through the tunnel

2.3. Layout of Test Work Points and Measuring Points. The test sites are as follows. The field dynamic test of the tunnel basement structure is carried out in the test tunnel, which mainly includes dynamic stress test and vibration acceleration test on the filling layer surface of the tunnel basement structure. The contents and number of points for the tunnel structure test are shown in Table 1.

Under the action of the test train, the dynamic strain and triaxial dynamic response (amplitude, strong vibration frequency, acceleration, and natural frequency) and other parameters of the tunnel basement structure are tested to master the working state of the tunnel structure under dynamic load.

The layout of measuring points is shown in Figure 1.

2.4. General Situation of Test Project. Three sections (cracked section, intact section, and repaired section) of a railway tunnel were selected for the structural dynamic test. The stress, vibration, safety, and other parameters of tunnel basement structure under the action of real vehicles were tested. The test site is shown in Figures 2–5.

2.5. Load Diagram of Test Locomotive. The test vehicle consists of one section of DF8B locomotive at the head and one at the tail, 21 sections of C80 special freight trucks (25-ton axle load), and 10 sections of C80E special freight trucks (27-ton axle load) in the middle. The load diagram is shown in Figures 6–8.

3. Analysis of Test Data

The vertical dynamic stress, vibration acceleration, and test data comparison of filling layer at tunnel basement structure have been analyzed in this section.

3.1. Vertical Dynamic Stress Analysis of Filling Layer at Tunnel Basement Structure. Taking this tunnel as an example, the vertical dynamic stress of the top surface of the invert filling layer in the intact zone, cracked zone, and repaired zone when the test train passes through is shown in Figures 9–11. The results show that the dynamic stress of DF8B locomotive is higher than that of C80E freight car, and the maximum vertical dynamic stress appears at the bogie of DF8B locomotive, which is 21.82 kPa, 33.91 kPa, and 31.70 kPa, respectively, showing an increasing trend. The average dynamic stress of C80 special truck is 11.25 kPa,

Table 1: Test contents and number of test points for tunnel structure test.

Serial number	Basement structure state	Line type	Sleeper type	Dynamic stress	X-axis vibration acceleration	Y-axis vibration acceleration	Z-axis vibration acceleration	Total
1	Cracked section	Heavy haul line	Concrete slab sleeper	6	4	4	4	18
2	Intact section			6	4	4	4	18
3	Repaired section			6	4	4	4	18
Total				18	12	12	12	54

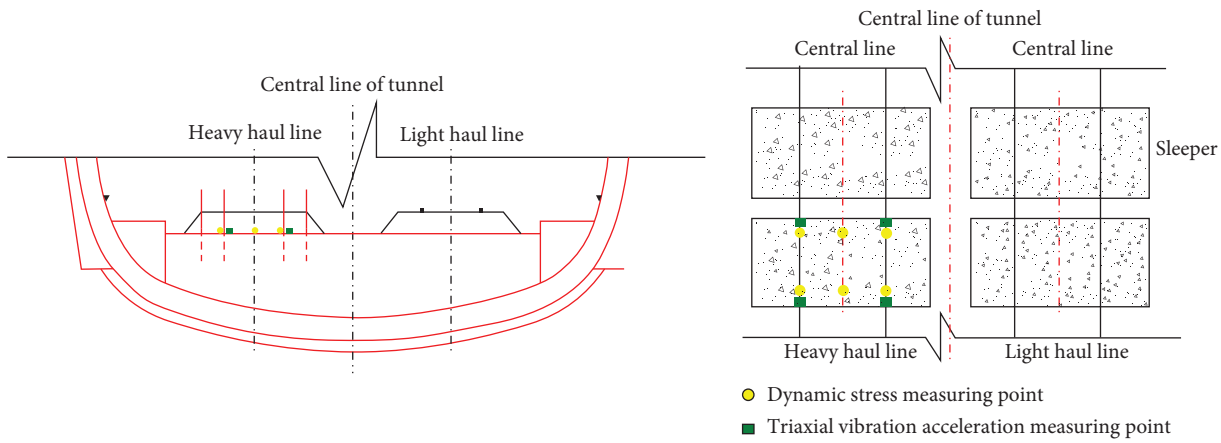

Figure 1: Layout of tunnel dynamic test points.

Figure 2: Field test site.

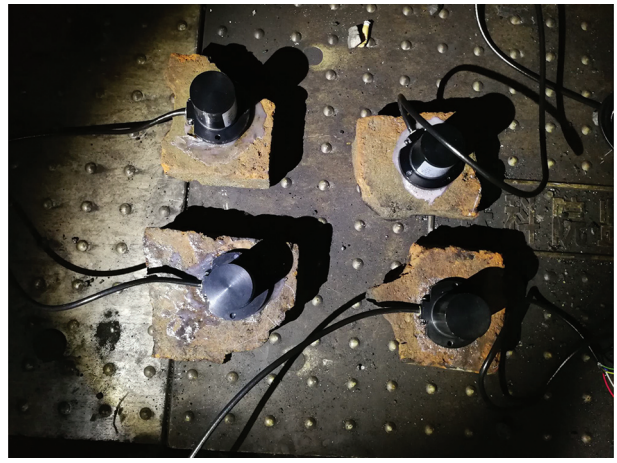

Figure 3: Fixing of three-axis vibration acceleration sensors.

30.84 kPa, and 28.37 kPa, which increases first and then decreases; the average dynamic stress of C80E special truck is 15.98 kPa, 31.09 kPa, and 29.07 kPa, which also increases first and then decreases.

The vertical dynamic stress of the top surface of the invert filling layer under the track of intact zone, cracked zone, and repaired zone when the test train passes through is shown in Figures 12–14. The results show that the dynamic stress of DF8B locomotive is higher than that of C80E special freight car, and the maximum vertical dynamic stress value appears at the bogie of the first section of C80E special freight car, which is 150.74 kPa, 154.12 kPa, and 152.14 kPa, respectively, which increases first and then decreases. The average dynamic stress of C80 special truck is 116.27 kPa, 120.74 kPa, and 117.47 kPa, respectively, which also increases first and then decreases; the average dynamic stress of C80E special truck is 139.33 kPa, 147.59 kPa, and 143.22 kPa, which also increases first and then decreases.

3.2. Vibration Acceleration Analysis of Filling Layer at Tunnel Basement Structure. Taking this tunnel as an example, the vibration accelerations of the top surface of the inverted arch filling layer directly below the track in the intact zone, which are perpendicular to the horizontal direction (X-axis), along the horizontal direction (Y-axis), and the vertical direction (Z-axis) of the line, are shown in Figures 15–17. The results show that the vibration acceleration of DF8B locomotive is

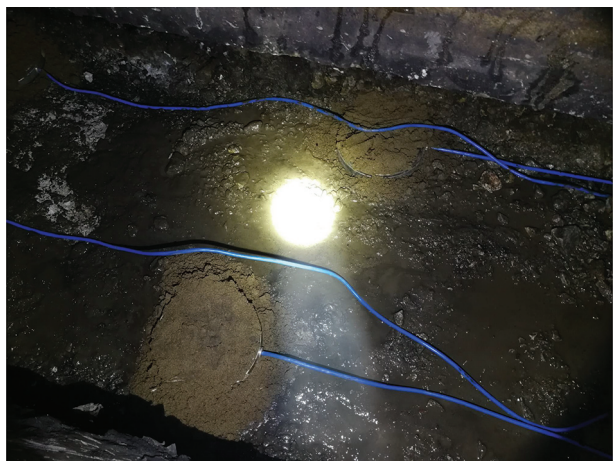

Figure 4: Installation of dynamic stress sensors.

Figure 5: Equipment commissioning.

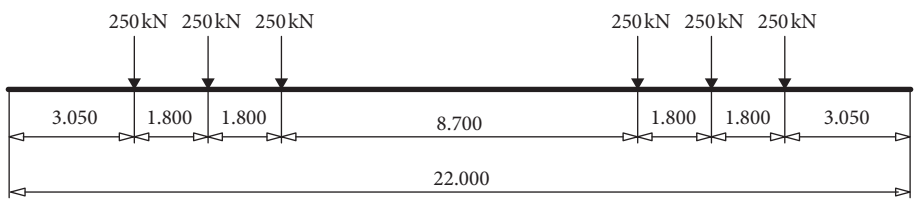

Figure 6: Load diagram of DF8B locomotive.

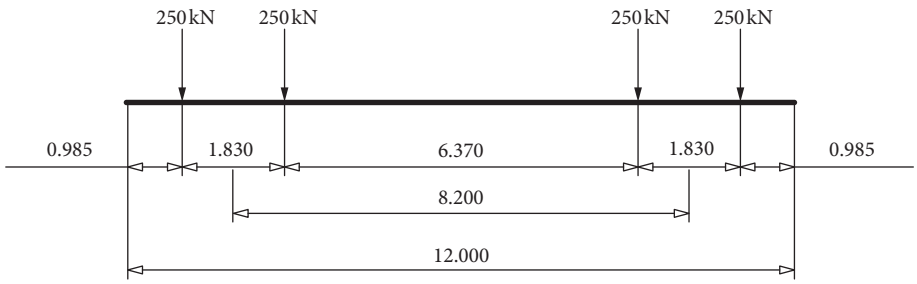

Figure 7: Load diagram of C80 special truck.

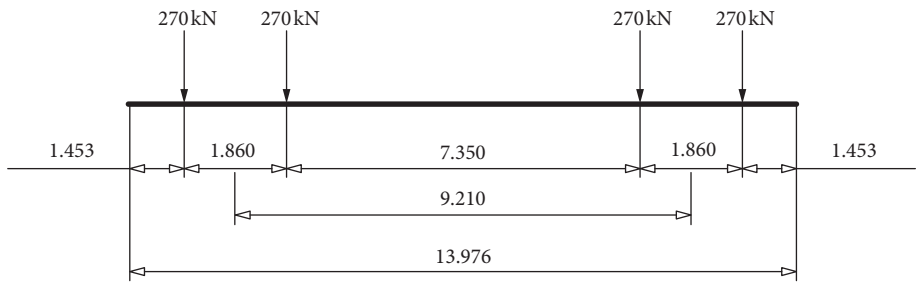

Figure 8: Load diagram of C80E special truck.

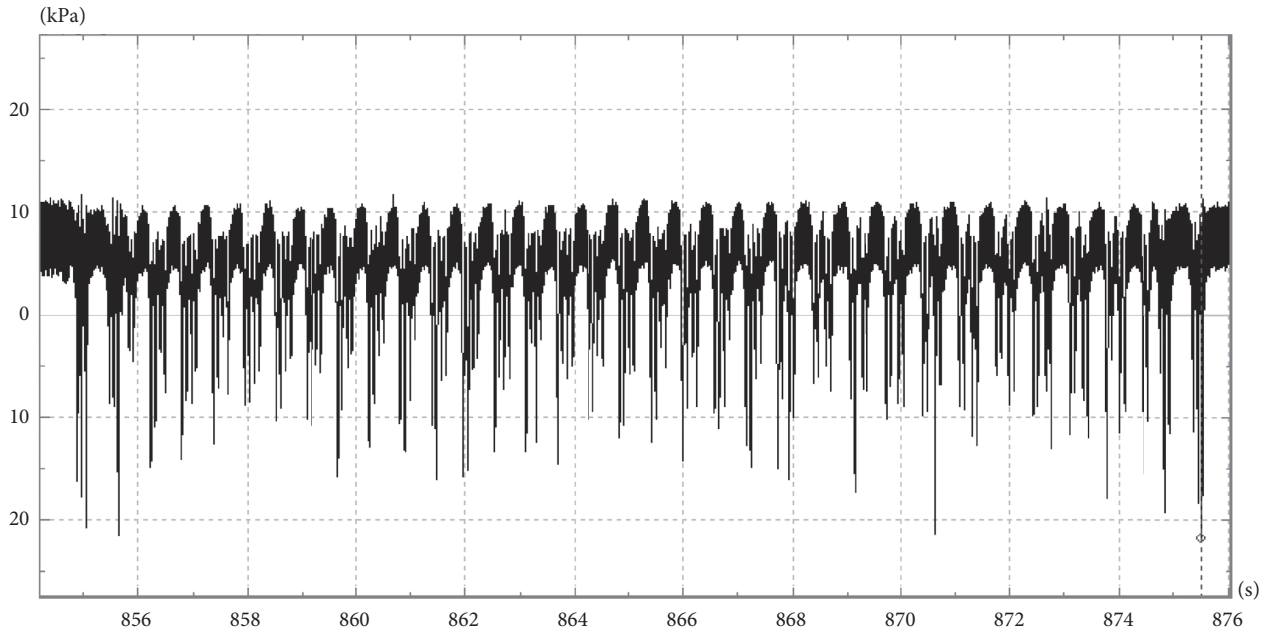

Figure 9: Vertical dynamic stress of the top surface of the invert filling layer in the intact zone.

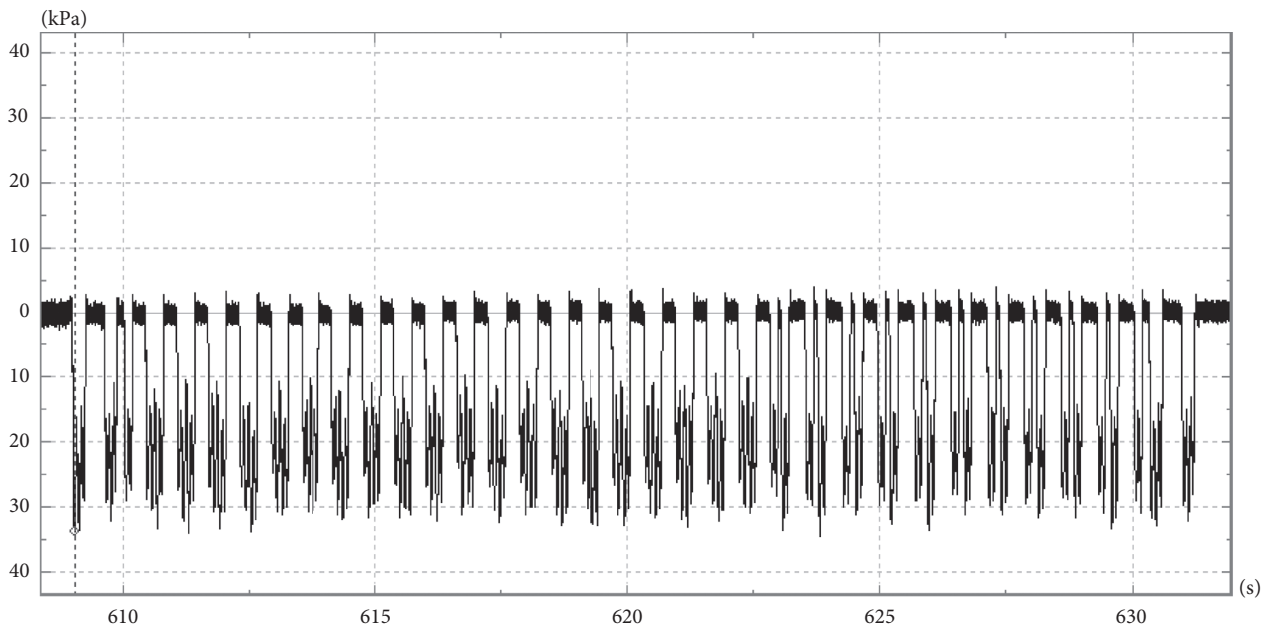

Figure 10: Vertical dynamic stress of the top surface of the filling layer of the wide inverted arch in the cracked zone.

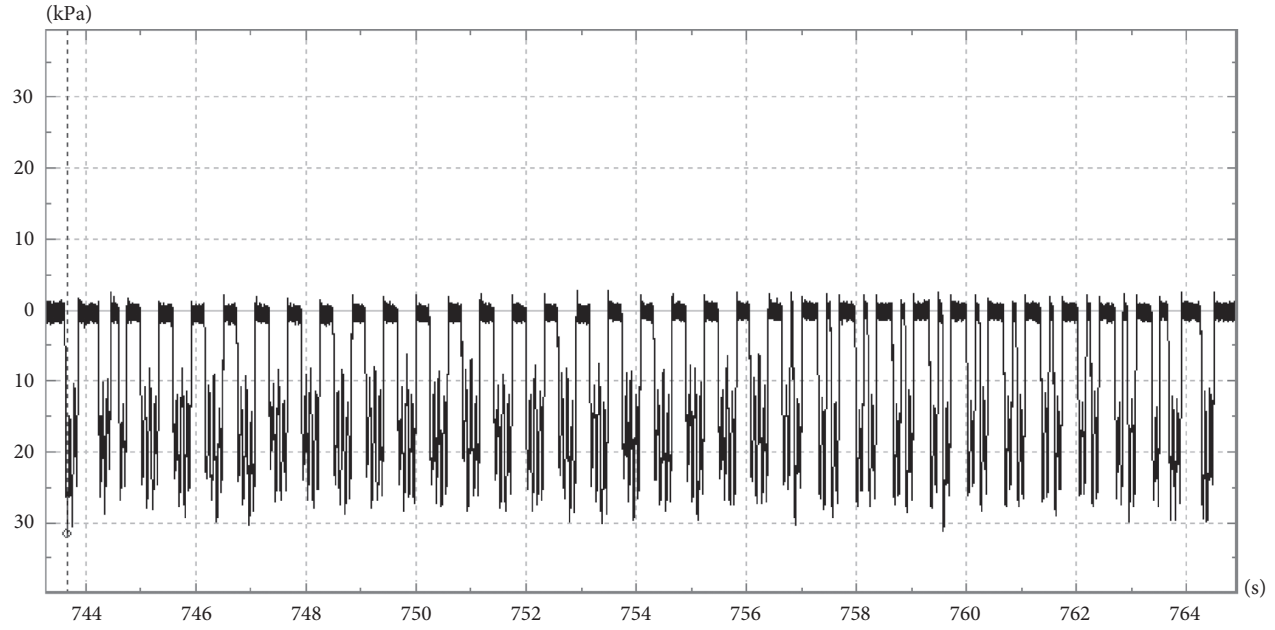

Figure 11: Vertical dynamic stress of track center on top of the invert filling layer in the repair zone.

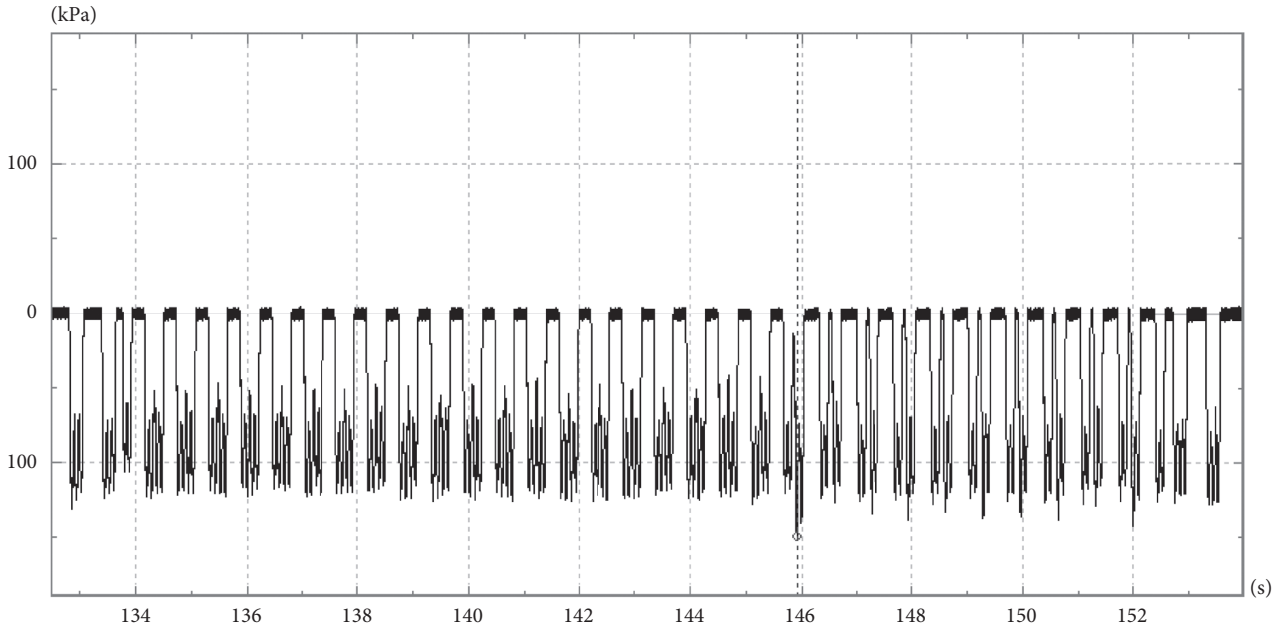

Figure 12: Vertical dynamic stress of the top surface of invert filling layer under the track in the intact zone.

higher than that of C80E special freight trucks. The order of vibration acceleration value of C80 special truck is vertical (Z-axis) > along the line horizontal (Y-axis) > vertical line horizontal (X -axis). The maximum vibration accelerations of vertical line horizontal (X-axis), along the line horizontal (Y-axis), and vertical (Z-axis) are 0.17 m/s^2, 1.77 m/s^2, and 2.41 m/s^2, respectively, showing an increasing trend. The results show that the average vibration accelerations of C80E special truck on the X-axis, Y-axis, and Z-axis are 0.05 m/s^2, 0.51 m/s^2, and 1.23 m/s^2, respectively, showing an increasing trend; the average vibration accelerations of C80E special truck on the X-axis, Y-axis, and z-axis are 0.03 m/s^2, 0.35 m/s^2, and 0.82 m/s^2, respectively, showing an increasing trend.

The vertical vibration acceleration (Z-axis) of the top surface of the inverted arch filling layer directly below the track in the cracked zone when the test train passes is shown in Figures 18-20. The results show that the order of vibration acceleration value of C80 special truck is (1) vertical (Z-axis) > along the line horizontal (Y-axis) > vertical line horizontal (X-axis); (2) crack zone > intact zone. The maximum vibration acceleration of vertical line in the horizontal direction (X-axis),

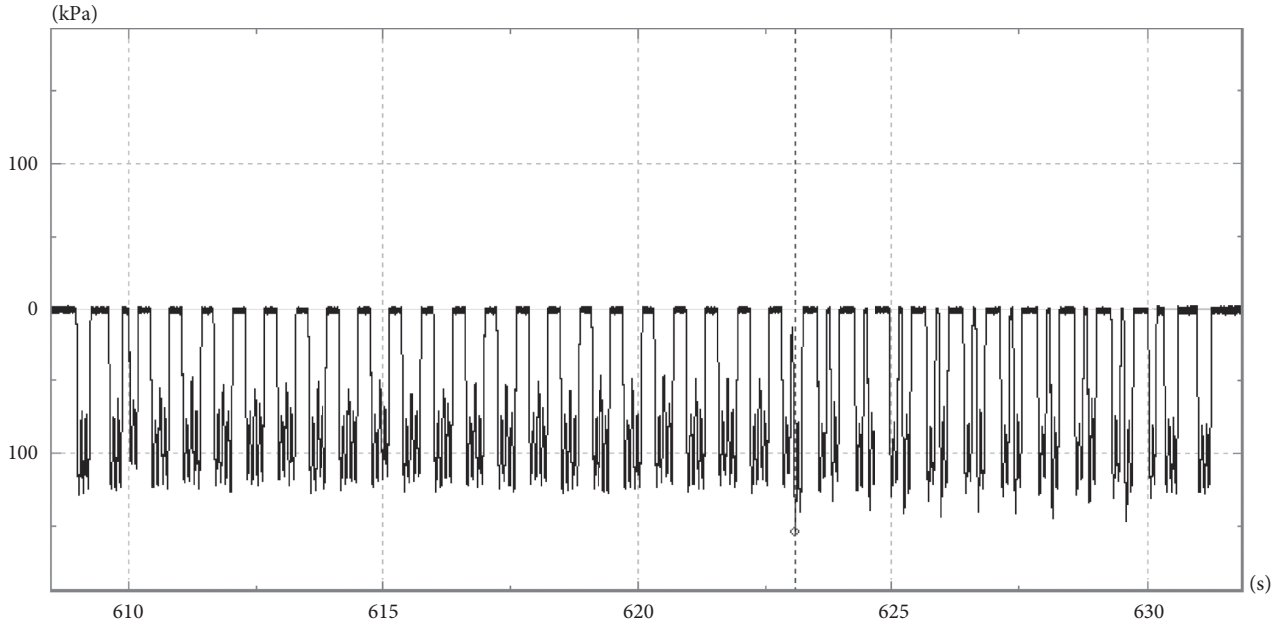

Figure 13: Vertical dynamic stress of the top surface of invert filling layer under the track in the cracked zone.

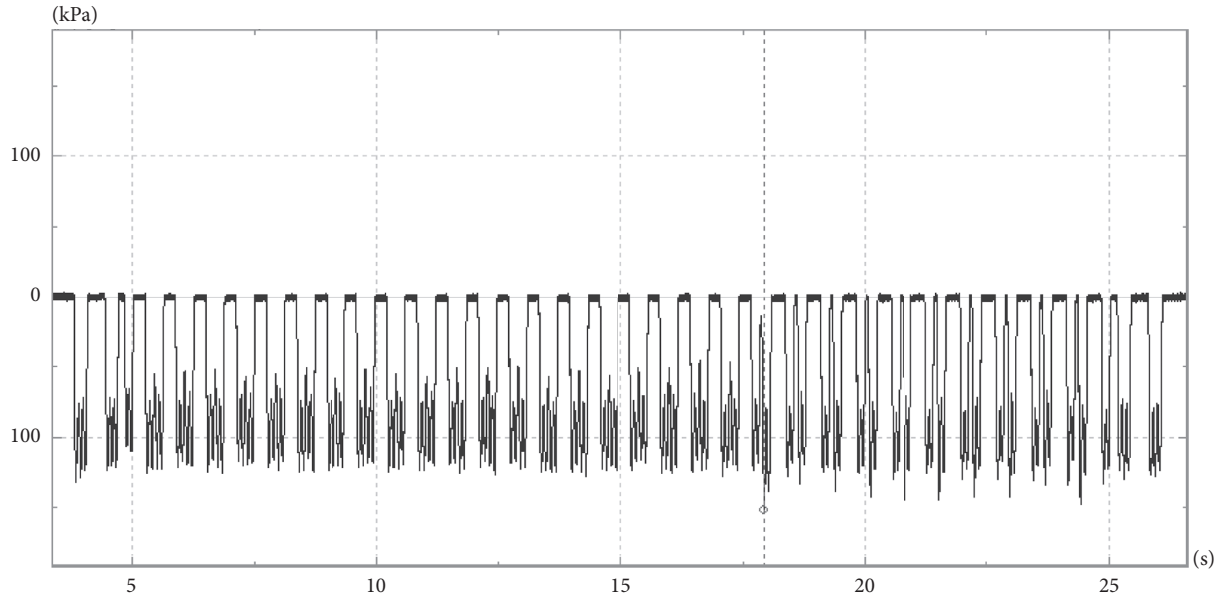

Figure 14: Vertical dynamic stress of the top surface of invert filling layer under the track in the repair zone.

horizontal (Y-axis), and vertical direction (Z-axis) is divided into three parts. The average vibration accelerations of C80E special truck on X-axis, Y-axis, and Z-axis are 3.21 m/s^2, 2.01 m/s^2, and 1.82 m/s^2, respectively; the average vibration accelerations of C80E special truck on X-axis, Y-axis, and Z-axis are 2.37 m/s^2, 1.97 m/s^2, and 1.95 m/s^2, respectively.

The vertical vibration acceleration (Z-axis) of the top surface of the inverted arch filling layer directly below the track in the repaired zone when the test train passes is shown in Figures 21–23. The results show that the vibration acceleration of DF8B locomotive is higher than that of C80E special freight trucks. The order of vibration acceleration value of C80 special truck in the repair zone is (1) vertical (Z-axis) > along the line horizontal (Y-axis) > vertical line horizontal (X-axis); (2) cracked zone > repaired zone > intact zone. The maximum vibration acceleration of C80E special truck is 0.15 m/s^2, 2.40 m/s^2, and 2.26 m/s^2, respectively; the average vibration acceleration of C80E special truck on X-, Y-, and Z-axes is 0.02 m/s^2, 0.48 m/s^2, and 0.37 m/s^2, respectively; the average vibration acceleration of C80E special truck on X-, Y-, and Z-axes is 0.01 m/s^2, 0.26 m/s^2, and 0.34 m/s^2, respectively.

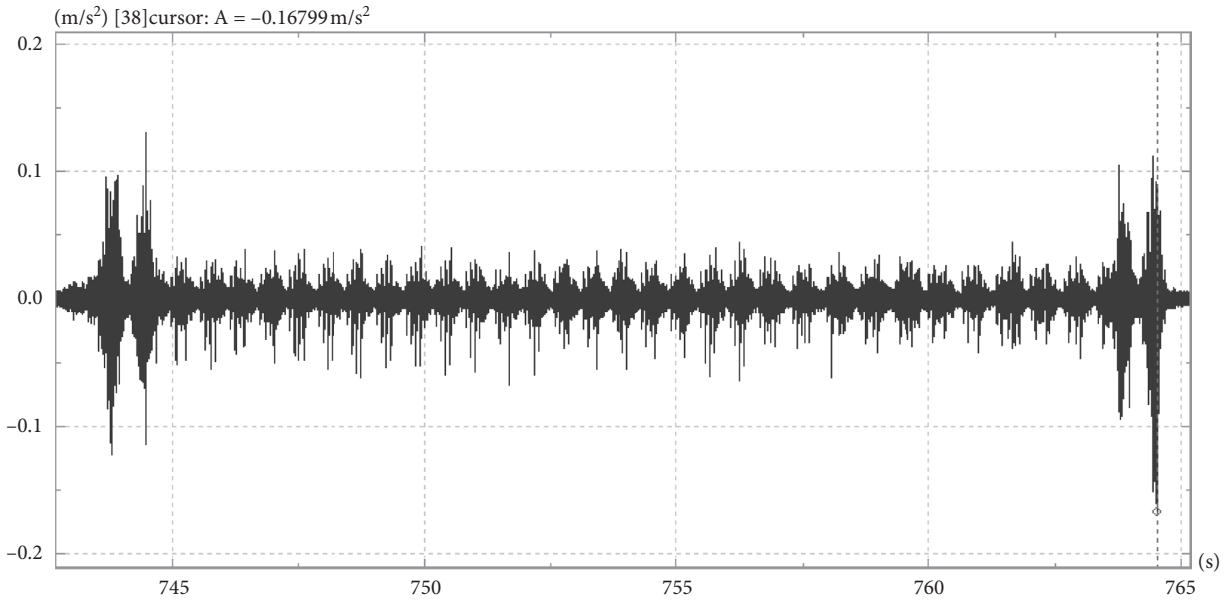

Figure 15: Time domain characteristic diagram of vibration acceleration along the line perpendicular direction (X-axis) in the intact zone.

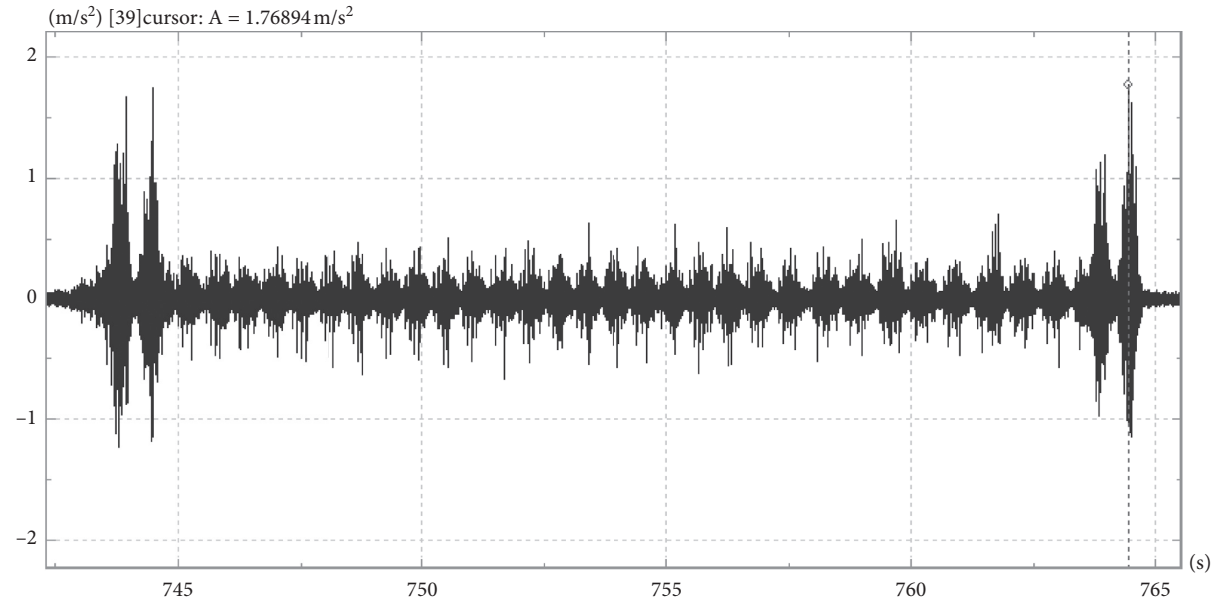

Figure 16: Time domain characteristic diagram of vibration acceleration along the line direction (Y-axis) in the intact zone.

3.3. Test Data Comparison. The distribution law of load along the tunnel structure was summarized, and the tunnel structure under the vibration load of the heavy haul train was mastered. The loading mode and dynamic performance of the system are discussed.'

3.3.1. Comparative Analysis of Test Data of Intact, A1 Level Crack, and Reinforced Sections. By comparing and analyzing the test data (as shown in Figures 24–26), such as the maximum vertical dynamic stress at the top of the inverted arch filling layer, the maximum vertical dynamic stress at the top of the inverted arch filling layer, and the maximum vertical acceleration at the top of the inverted arch filling layer under the track in the intact section, the A1 level cracked section, and the reinforced section, the following rules are obtained:

(i) The maximum vertical dynamic stress on the top of the inverted arch filling layer directly below the track is A1 level crack section > reinforcement section > intact section

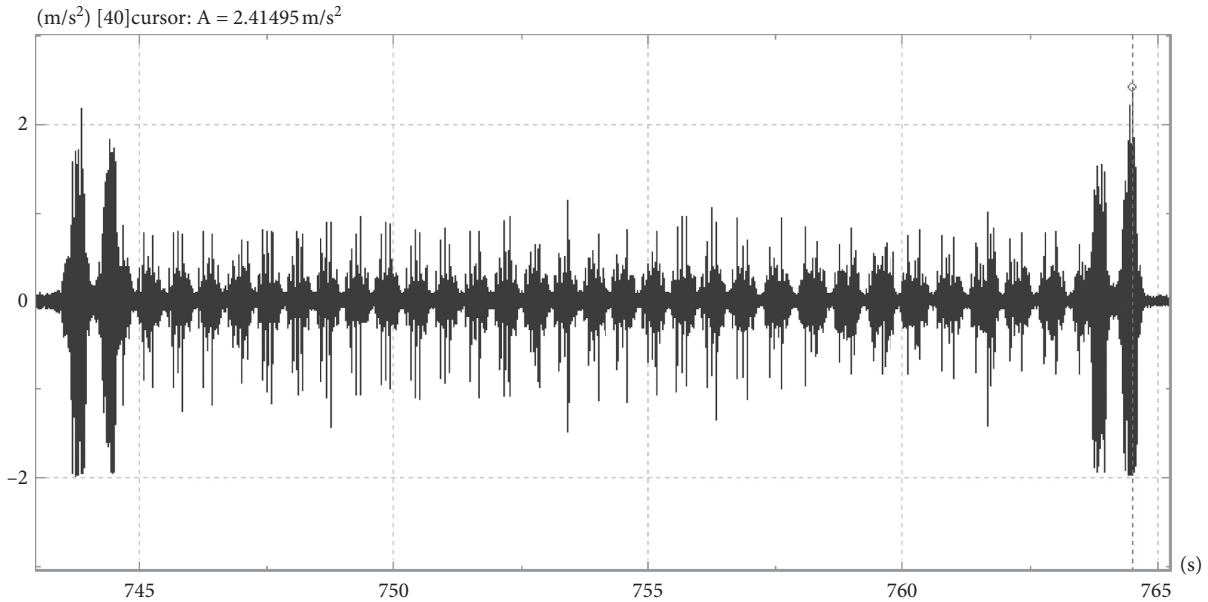

Figure 17: Time domain characteristic diagram of vibration acceleration along the vibration direction (Z-axis) in the intact zone.

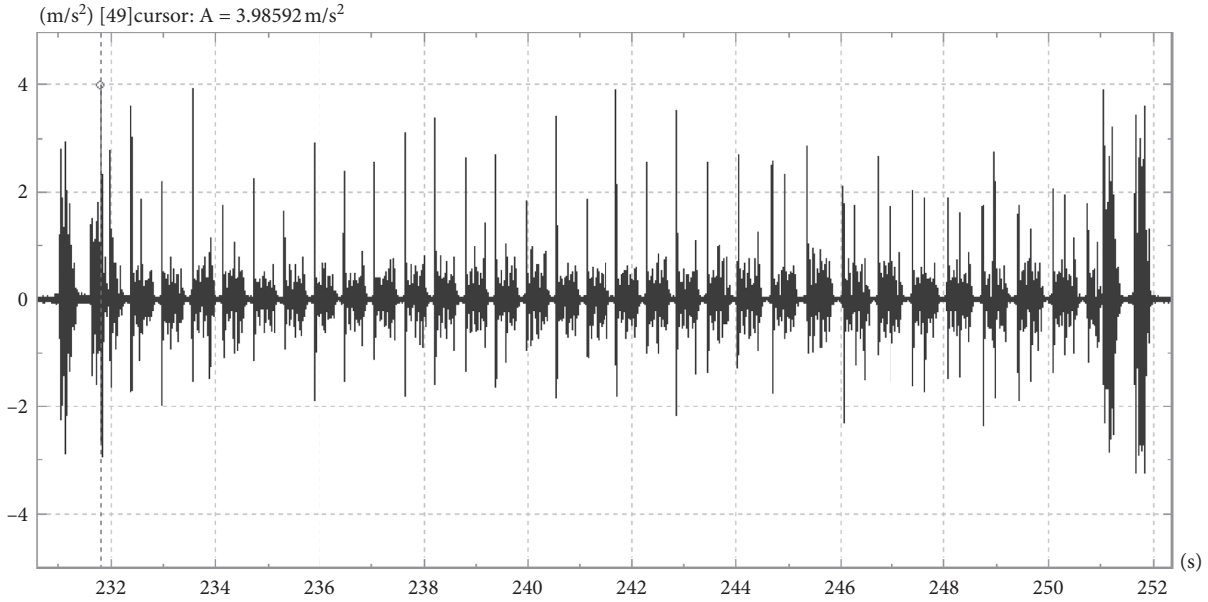

Figure 18: Time domain characteristic diagram of vibration acceleration along the line perpendicular direction (X-axis) in the fracture zone.

(ii) The maximum vertical dynamic stress at the top of the filling layer is A1 level crack section > reinforcement section > intact section

(iii) The maximum vertical vibration acceleration of the top surface of the inverted arch filling layer directly below the track is A1 level crack section > intact section > reinforced section

3.3.2. Comparative Analysis of Test Data of DF8B, C80, and C80E. By comparing and analyzing the test data at the centre of the road on the top of the inverted arch filling layer and the maximum vertical dynamic stress value of the inverted arch filling layer under the track of DF8B locomotive, C80 special freight trucks (25-ton axle load), and C80E general freight trucks (27-ton axle load), the following rules are obtained:

(i) The maximum vertical dynamic stress at the centre of the road on the top of the inverted arch filling layer: DF8B locomotive > C80E general purpose freight trucks (27-ton axle load) > C80 special purpose freight trucks (25-ton axle load).

(ii) The maximum vertical dynamic stress on the top of the inverted arch filling layer directly below the track: DF8B locomotive > C80E general purpose

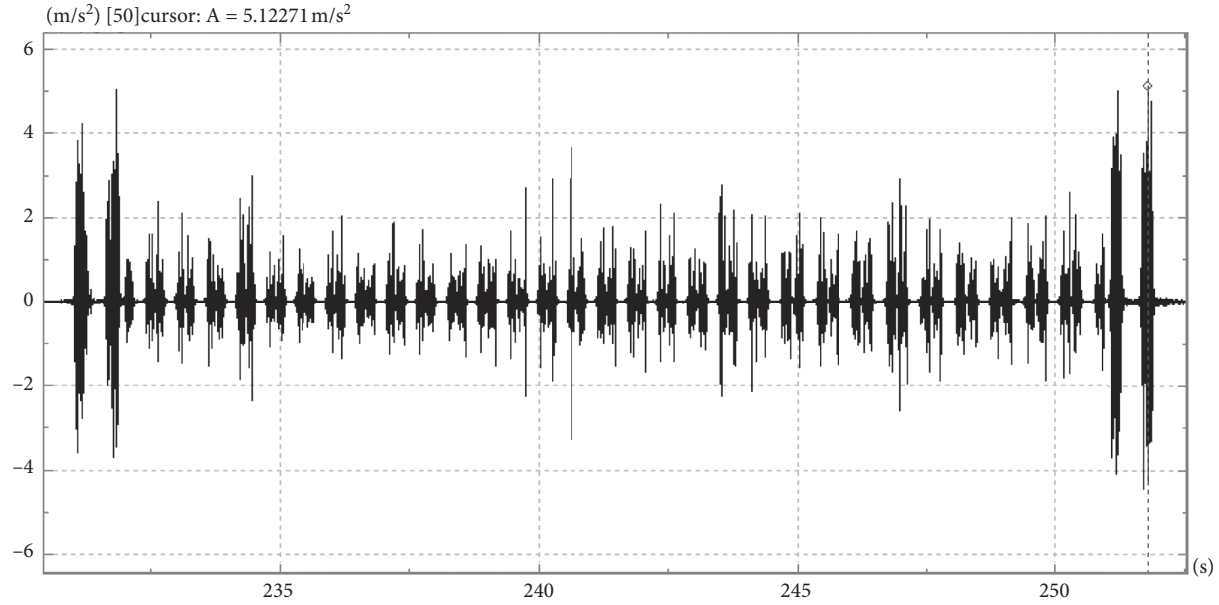

Figure 19: Time domain characteristic diagram of vibration acceleration along the line direction (*Y*-axis) in the fracture zone.

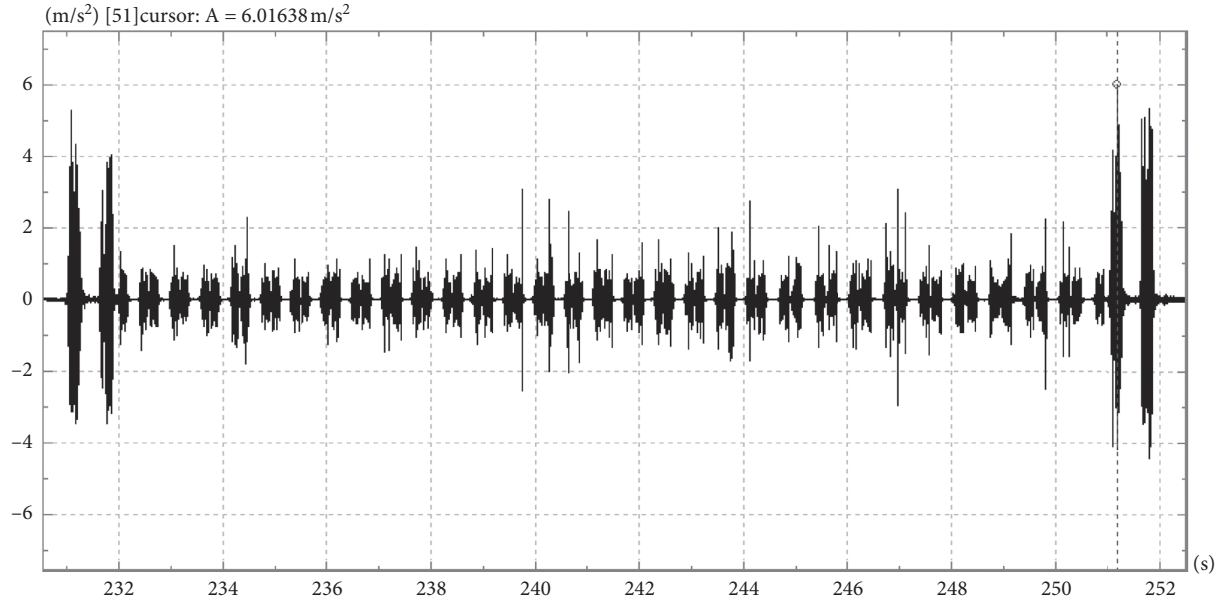

Figure 20: Time domain characteristic diagram of vibration acceleration along the vibration direction (*Z*-axis) in the fracture zone.

freight trucks (27-ton axle load) > C80 special purpose freight trucks (25-ton axle load).

(ii) The vertical vibration acceleration of the intact section: DF8B locomotive > C80 special freight trucks (25-ton axle load) > C80E general freight trucks (27-ton axle load).

(iii) The vertical vibration acceleration of the A1 level cracked section: DF8B locomotive > C80 special freight trucks (25-ton axle load) > C80E general freight trucks (27-ton axle load).

(iv) Thevertical vibration acceleration of the reinforced section: DF8B locomotive > C80 special

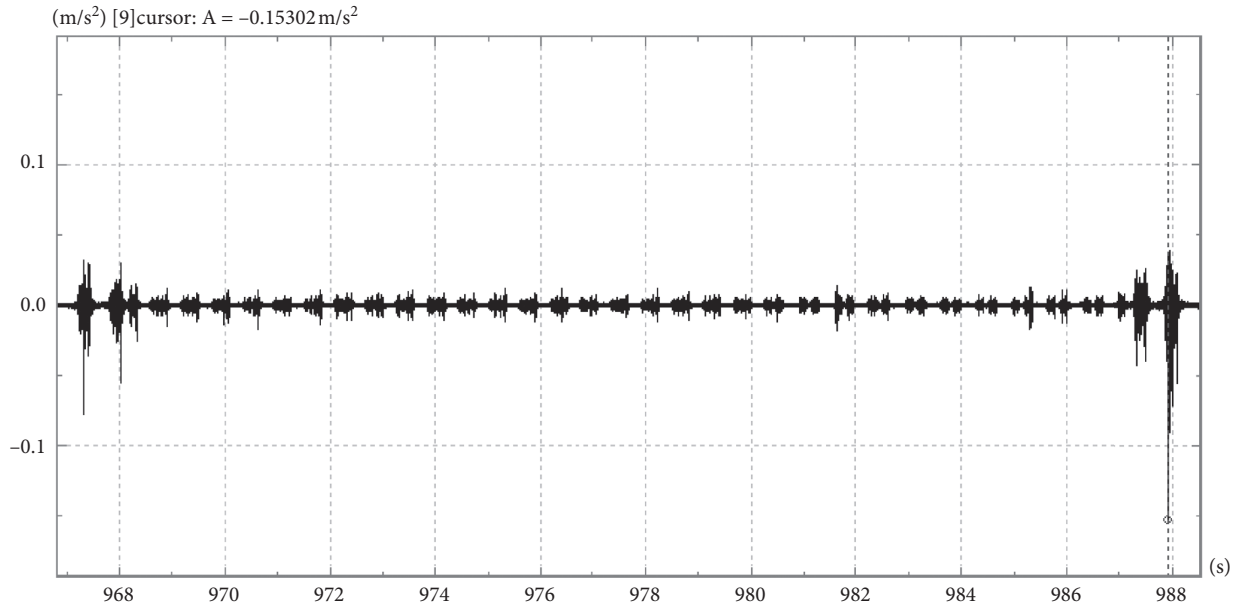

Figure 21: Time domain characteristic diagram of vibration acceleration along the line perpendicular direction (X-axis) in the repair zone.

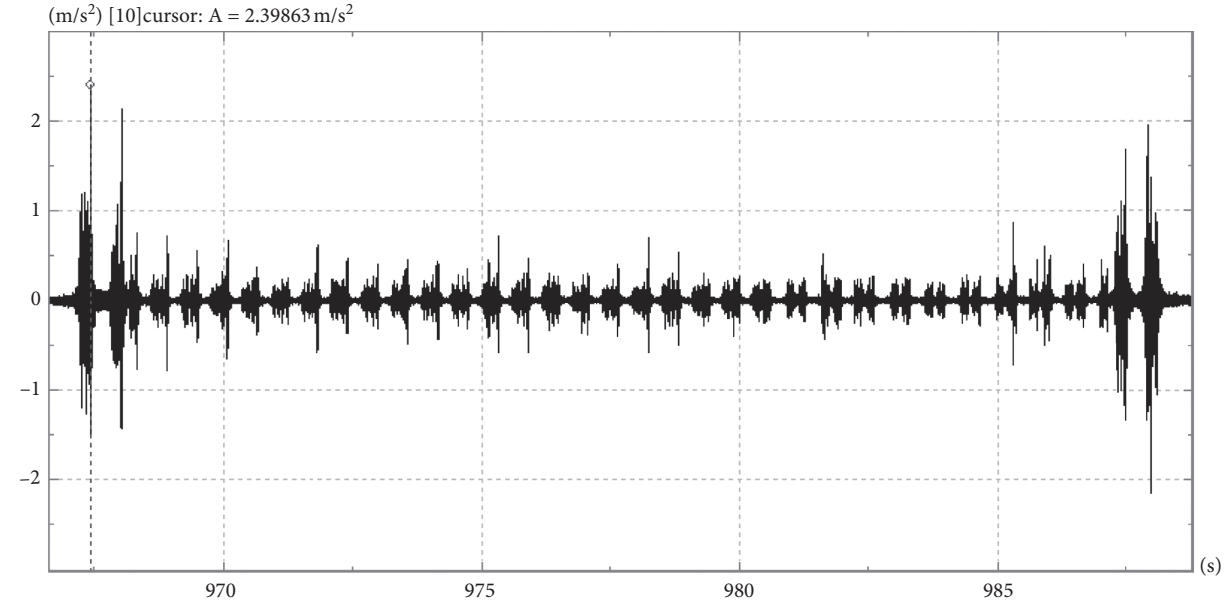

Figure 22: Time domain characteristic diagram of vibration acceleration along the line direction (Y-axis) in the repair zone.

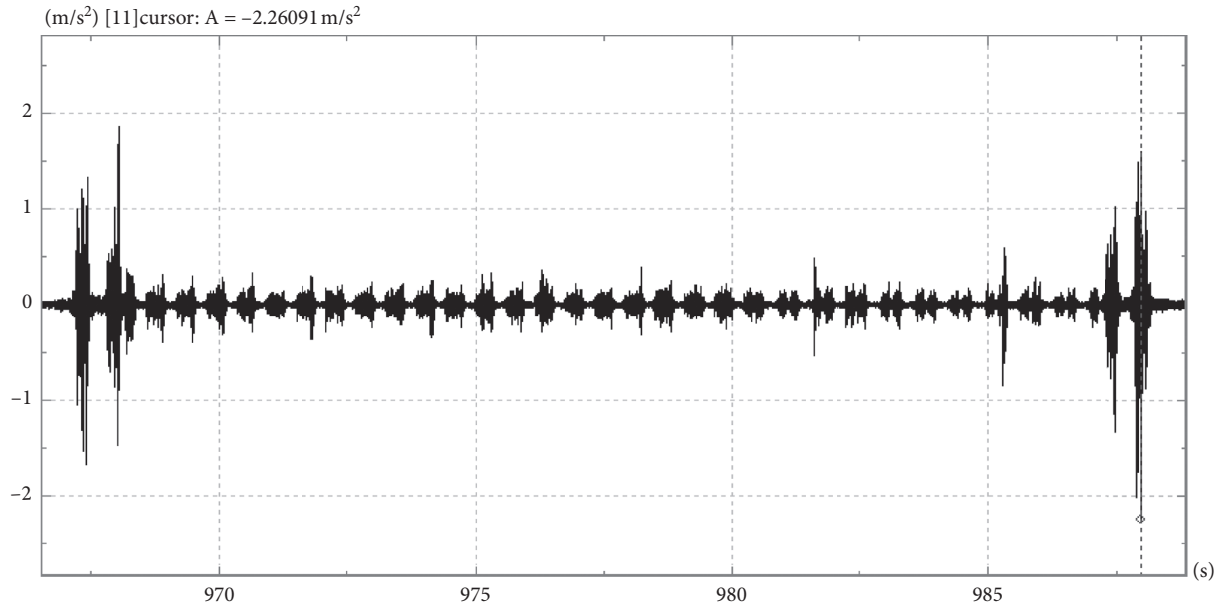

Figure 23: Time domain characteristic diagram of vibration acceleration along the vibration direction (Z-axis) in the repair zone.

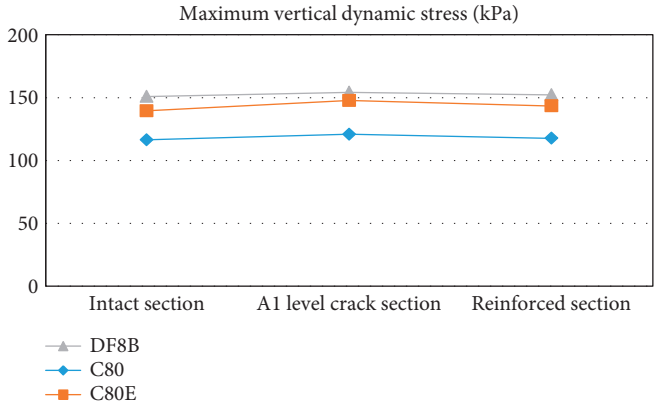

Figure 24: Comparative analysis diagram of maximum vertical dynamic stress on the top surface of filling layer under the rail.

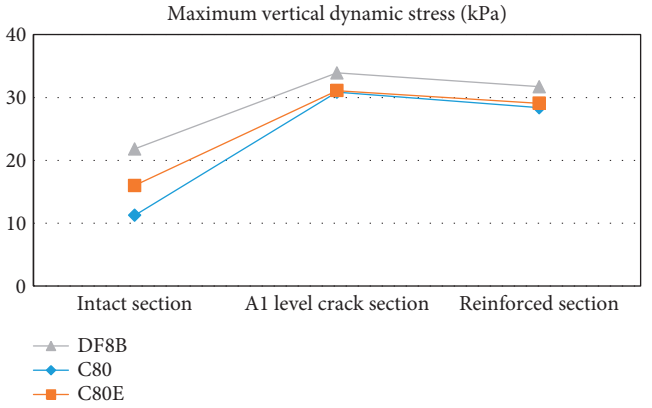

Figure 25: Comparative analysis of maximum vertical dynamic stress on top surface of filling layer between two rails.

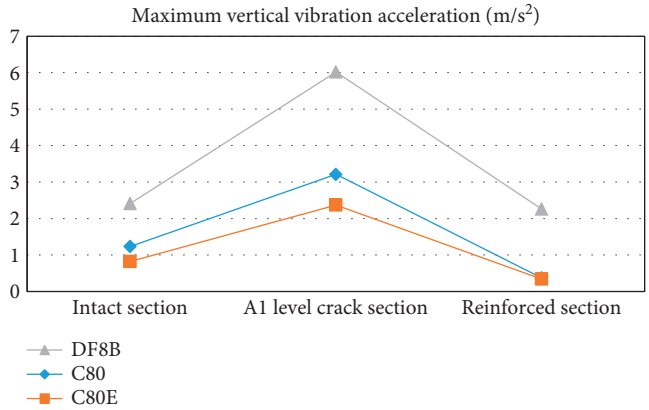

Figure 26: Comparative analysis diagram of maximum vertical acceleration between two rails on the top surface of filling layer under the rail.

truck (25-ton axle load) > C80E general truck (27-ton axle load).

4. Conclusion

By analyzing the influence law of dynamic response and fatigue life of heavy haul train under different basement conditions (intact, damaged, and repaired), the adaptability of the railway tunnel equipment to freight trucks axle load is clarified.

(1) The intact section of the tunnel can meet the normal operation of 25-ton and 27-ton axle load freight trains in good condition.

(2) The normal operation of 25-ton and 27-ton axle load freight trucks is seriously affected by the cracked section of the tunnel. When the cracks in the tunnel basement are gradually hollowed out by groundwater, serious traffic accidents such as vehicle shaking and derailment are likely to occur.

(3) The repaired section of the tunnel can meet the normal operation of 25-ton and 27-ton axle load freight trains after adopting the integrated comprehensive treatment of "Anchor-Injection-Drainage".

Data Availability

The data used to support the findings of this study are available within the article.

Conflicts of Interest

The authors declare that there are no conflicts of interest regarding the publication of this article.

Acknowledgments

The authors are grateful for the support of the Research and Development Project of Science and Technology of China Railway Corporation (no. P2018X011).

References

[1] J. Lai, K. Wang, J. Qiu, F. Niu, J. Wang, and J. Chen, "Vibration response characteristics of the cross tunnel structure," *Shock and Vibration*, vol. 2016, Article ID 9524206, 16 pages, 2016.

[2] W. Garden and H. G. Stuit, "Modelling of soil vibrations from railway tunnels," *Journal of Sound and Vibration*, vol. 267, no. 1, pp. 605–619, 2003.

[3] A. V. Metrikine, A. C. W. M. Vrouwenvelder, Y. Q. Liu, and W. B. Ma, "Surface ground vibration due to a moving train in a tunnel: two-dimensional model," *Journal of Sound and Vibration*, vol. 234, no. 1, pp. 43–66, 2000.

[4] T. Balendra, C. G. Koh, and Y. C. Ho, "Dynamic response of buildings due to trains in underground tunnels," *Earthquake Engineering & Structural Dynamics*, vol. 20, no. 3, pp. 275–291, 1991.

[5] G. Degrande, M. Schevenelsa, P. Chatterjeea et al., "Vibrations due to a test train at variable speeds in a deep bored tunnel embedded in London clay," *Journal of Sound and Vibration*, vol. 293, no. 1, pp. 626–644, 2006.

[6] Y. B. Yang and H. H. Hung, "Soil vibrations caused by underground moving trains," *Journal of Geotechnical and Geoenviromental Engineering*, vol. 134, no. 1, pp. 1633–1644, 2008.

[7] S. Wu, Z. Wu, and C. Zhang, "Rock burst prediction probability model based on case analysis," *Tunnelling and Underground Space Technology*, vol. 93, Article ID 103069, 2019.

[8] S. Wu, L. Han, Z. Cheng, X. Zhang, and H. Cheng, "Study on the limit equilibrium slice method considering characteristics of inter-slice normal forces distribution: the improved Spencer method," *Environmental Earth Sciences*, vol. 78, no. 20, p. 611, 2019.

[9] S. Wu, S. Zhang, C. Guo, and L. Xiong, "A generalized nonlinear failure criterion for frictional materials," *Acta Geotechnica*, vol. 12, no. 6, pp. 1353–1371, 2017.

[10] S. Wu, H. Wu, and J. Kemeny, "Three-dimensional discrete element method simulation of core disking," *Acta Geophysica*, vol. 66, no. 3, pp. 267–282, 2018.

[11] W. B. Ma, J. F. Chai, Z. L. Han et al., "Research on design parameters and fatigue life of tunnel bottom structure of single-track ballasted heavy-haul railway tunnel with 40-ton axle load," *Mathematical Problems in Engineering*, vol. 2020, Article ID 3181480, 9 pages, 2020.

[12] Z. Tao, C. Zhu, M. He, and M. Karakus, "A physical modeling-based study on the control mechanisms of Negative Poisson's ratio anchor cable on the stratified toppling deformation of anti-inclined slopes," *International Journal of Rock Mechanics and Mining Sciences*, vol. 138, Article ID 104632, 2021.

[13] C. Zhu, M. He, M. Karakus, X. Zhang, and Z. Tao, "Numerical simulations of the failure process of anaclinal slope physical model and control mechanism of negative Poisson's ratio cable," *Bulletin of Engineering Geology and the Environment*, vol. 80, no. 4, pp. 3365–3380, 2021.

[14] L. Han, C. Chen, T. Guo et al., "Probability-based service safety life prediction approach of raw and treated turbine blades regarding combined cycle fatigue," *Aerospace Science and Technology*, vol. 110, 2021.

[15] L. Han, Y. B. Wang, Y. Zhang, C. Lu, C. Fei, and Y. Zhao, "Competitive cracking behavior and microscopic mechanism of Ni-based superalloy blade respecting accelerated CCF failure," *International Journal of Fatigue*, vol. 150, Article ID 106306, 2021.

[16] Y. Wang, "History of the republic of china railway: datong-qinhuangdao heavy haul railway," *Archives Spring and Autumn*, vol. 2019, no. 4, pp. 10–14, 2019.

[17] D. W. Zhang, "Investigation and suggestions on diseases of key tunnels on Datong Qinhuangdao railway," *Railway Standard Design*, vol. 2002, no. 4, pp. 32–34, 2002.